Synthesis, characterization of GO-zinc oxide nanocomposites and their use as an adsorbent for the removal of organic dyes in industrial effluents

H. Rehman[a], Z. Ali[b,*] T. G. Shahzady[c], A. Zahra[d], H. Hussain[e], A. Anwar[b], M.S. Latif[c]

[a]*Department of Chemistry, University of Sahiwal, Sahiwal, Pakistan*
[b]*Department of Basic Sciences & Humanities, University of Engineering & Technology Lahore New Campus, Pakistan*
[c]*Department of Chemistry, Lahore Garrison University, DHA Lahore, Pakistan*
[d]*Govt College for women, Jhang, Pakistan*
[e]*Department of Basic Sciences & Humanities, University of Engineering & Technology Lahore Narowal Campus, Pakistan*

In this investigation, GO-ZnO nanocomposites were synthesized by using hydrothermal method. The structure, morphology and optical properties of synthesized nanocomposites were analyzed through Fourier transformed infrared spectroscopy (FTIR), X-ray diffraction (XRD), Scanning electronic microscopy (SEM), and UV-Visible spectroscopy. The XRD pattern confirmed the formation of Graphene decorated with hexagonal ZnO with high crystallinity. SEM revealed that the graphene paternity image decorated ZnO uniformly. UV-Visible spectroscopy was utilized to study photocatalytic degradation of synthesized materials against rhodamine B and methyl blue dyes and good catalytic activity was observed for both samples. Graphene-ZnO nanocomposites showed higher catalytic activity than ZnO nanoparticles.

(Received August 31, 2021; Accepted November 27, 2021)

Keywords: Graphene-ZnO nanocomposites, Adsorbent, Organic dyes

1. Introduction

Nowadays, pollution of water resources by dyes or dye-based effluent discharged from many industries is already a worldwide problem. Today, across the world there are more than 10,000 commercially available dyes with over 7×10^5 tonnes of them being annually synthesized [1]. Non-biodegradable and toxic nature of most of these synthesized dyes affects water quality at as little concentration as 1 ppm [2, 3] which poses great environmental concern. Thus, it's of great importance, that these dyes should be effectively removed from aqueous systems. Over the past years a large number of processes have been used for the removal of dyes from wastewater such as biological, chemical precipitation, coagulation/ flocculation, membrane filtration, ion exchange, electrochemical destruction and adsorption [4, 5]. As all these techniques are non-destructive, so these techniques need further treatment [6, 7]. In order to remove organic pollutants and toxic chemicals in the waste water, use of nanoparticles has attained greater attention due to their greater adsorption activity and potent catalytic activity [8, 9]. As compare to other NPs use of magnetic NPs and their composites are considered to be more effective for water treatment, because of their ease in recovery from the solution using magnetic attraction[10,11].Therefore in order to aid this recovery composite formation , by impregnating these NPs on an adsorbate is much popular now a days . Moreover these composites, if composed of organic and inorganic sites, have various kinds of active sites, so behave as potent adsorbents for adsorbing pollutants [12].

Among nanocomposite adsorbents, ZnO composites have been reported to be highly efficient for treatment of dye polluted water [13-19]. ZnO composites in combination of other materials like chitosan, graphene, graphene oxides, plyaniline and clay minerals are frequently used [20-24]. This study reports the synthesis of GO-ZnO nancomposites for the removal of organic dyes in industrial effluents.

Corresponding author: zulfiqarali@uet.edu.pk

2. Experimental

2.1. Materials

Precursors used in this work are Graphite Powder, 37% Hydrochloric acid (HCl), 98% Sulfuric acid (H_2SO_4), Hydrogen Peroxide (H_2O_2), Potassium Permanganate ($KMnO_4$), Sodium Nitrate ($NaNO_3$), Zinc Nitrate Hexahydrate ($ZnNO_3.6H_2O$), Absolute Ethanol, Potassium Hydro-Oxide. All these chemicals were obtained from Sigma Aldrich and used without any further purification.

2.2. Synthesis of grapheme oxide nanoparticles by Modified Hummer's Method:

GO was synthesized from graphite fine powder by following modified Hummer's method [25, 26]. In this method 4 g of graphite powder, 2 g $NaNO_3$ were mixed in 200 ml of H_2SO_4 (98%) in 1000 ml of volumetric flask and placed in ice bath at (0-5 °C) for 1 hour with continuous stirring. When 1 hour continuous stirring caused suspension in the flask, then 10 g $KMnO_4$ was slowly added into the suspension and again stirred for 1 hour under similar conditions. The ice bath was then removed; the flask was placed on hot magnetic stirrer (35°C) until it became pasty brownish and kept under stirring for 2 hours. It was then subsequently diluted with slow addition of 400 ml water. The reaction temperature was rapidly increased to 98°C and the reaction mixture adopted brown colour. The reaction mixture was further diluted by 200 ml of water and stirred continuously. Finally the solution was treated with 20 ml H_2O_2 (30 % aqueous solution) to complete the oxidation and reduction reactions by appearance of yellow colour. The reaction product was centrifuged and washed with deionised water and 10% HCl solution repeatedly. Finally the product GO was obtained as a powder by drying it under vacuum at room temperature.

2.3. Preparation of Graphene-ZnO nanocomposites:

M. Saranya et al [27] method with slight modification was used in which 0.2 g GO was re-dispersed in 50 ml solution of ethanol and de ionized water (2:3) under sonication for 30 min. Zn $(NO_3)_2.6H_2O$ was added to the GO arrangement and mixed for 15 minutes to deliver a uniform dispersion. Dil. NaOH was then added to the blend till a pH of 12 is acquired and stirred for 30 min. The blend was then transferred to a 50 ml Teflon stain less steel autoclave and put in an oven for 10 hours at 90^{o}C. The precipitates of Gr-ZnO nanocomposite was segregated from this solution by centrifugation, washed several times with water, ethanol individually and dried over night in an oven at 70^{o}C temperature.

Proposed Reaction Mechanism:

$$\text{Graphite Powder} + H_2SO_4 + KMnO_4 + H_2O_2 \longrightarrow GO + SO_x + H_2O$$

$$GO + Zn(NO_3)_2.6H_2O + 2NaOH \longrightarrow GO + Zn(OH)_2 + 2NaNO_3 + 6H_2O$$

$$Zn(OH)_2 + 2H_2O \longrightarrow Zn^{+2} + 2OH^{-1} + 2H_2O$$

$$GO + Zn^{+2} + 2OH^{-1} + 2H_2O \longrightarrow GO\text{---}Zn(OH)_4 + 2H^{+1}$$

$$GO\text{---}Zn(OH)_4 \longrightarrow \underset{\textit{Nanocomposite}}{GO\text{---}ZnO} + H_2O + 2OH^{-1}$$

2.4. Photocatalytic Degradation Experiment

2.4.1. Preparation of Stock Solutions:

Stock solutions of two organic dyes i.e Rhodamine B and Methylene blue were prepared by dissolving 1 g of commercially available dyes (Fluka grade) in 1 L of distilled water. The resultant stock solution has concentration of 1000 mg/L. Standard solutions of desired concentrations were prepared by appropriate dilution of stock solutions.

2.4.2. Evaluation of photocatalytic activity:

Photocatalytic activity of ZnO and Gr-ZnO nanocomposite were evaluated against RhB and MB dyes under UV light illumination at 565-660 nm [28]. In photocatalytic test, 2.5mg of ZnO/Gr-ZnO nanocomposite catalyst was added to 50 ml dye solution (10μg/ml) and magnetically stirred for 30 min. In order to provide foundation of an adsorption/desorption equilibrium between the dye and photocatalyst, 120 min are provided before UV light irradiation. 5 ml aliquot was filtrated to remove the catalyst particles before measuring the absorbance using UV-Vis spectrophotometer.

3. Results and Discussion

Composite materials based on Graphene were investigated in recent time due to its large number of applications. Zinc Oxide is an interesting semiconducting material and its photocatalysts are frequently used for solving environmental issues. The photocatalytic property of metal oxides is greatly enhanced when it is fused with carbon containing material like grapheme. Synthesized materials can be characterized by following various techniques.

3.1. FTIR analysis

The FTIR spectra of Graphene Oxide and Gr-ZnO nanocomposite are shown in Figure 3.1.

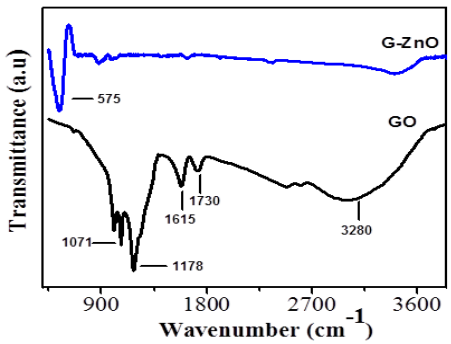

Fig. 1. FTIR of Graphene Oxide and Gr-ZnO nanocomposites.

A broad peak appeared at 3280 cm^{-1} in the high frequency area attributed to the stretching mode of O-H bond [29] and reveals the presence of hydroxyl groups in graphene oxide. The band observed at 1730 cm^{-1} was assigned to the carboxyl group [30, 31]. The sharp peak found at 1615 cm^{-1} is a resonance peak that can be assigned to the stretching and bending vibration of OH groups of water molecules adsorbed on graphene oxide. The peak at 1178 cm^{-1} represents C-O-C stretching and the peak at 1071 cm^{-1} corresponds to the vibrational mode of the C-O group [32].

In synthesis of Gr-ZnO nancompsite, removal of oxygen in thermal reduction process of Graphene oxide can be proved by disappearing –OH peak in its spectrum. It is a great evidence of formation ZnO nanocompsite on the surface of Graphene Oxide. A significant and strong peak at 575 cm^{-1} is attributed to ZnO nanoparticles [33].

3.2. XRD analysis

3.2.1. Graphene oxide

X-ray diffraction is a technique which contributes detail information about the chemical composition and crystallographic structure of the materials. It is also a unique tool used to detect the presence of phases in the material. To obtain the structural information about GO, X-ray analysis was done. Various diffraction lines were observed in XRD pattern, in which one prominent diffraction peak centred at $2\theta/^{0}$ =10.8 having (111) miller indices can be noticed. Appearance of this peak indicated the complete oxidation of graphite into GO as shown in Figure 2.

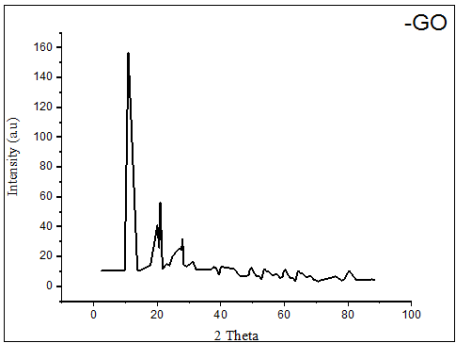

Fig. 2. XRD Pattern of GO-NP.

Table 1. Claculation of Miller Indices through Xrd Diffraction Pattern of GO-NPs.

2θ/⁰	**θ/⁰**	**$Sin^2\theta$**	**1x $\frac{Sin^2\theta}{Sin^2\theta_{min}}$**	**2x $\frac{Sin^2\theta}{Sin^2\theta_{min}}$**	**3x $\frac{Sin^2\theta}{Sin^2\theta_{min}}$**	**Whole integers**	***Hkl***
10.8908	5.4454	0.0090	1	2	3	3	111
20.1314	10.0657	0.0305	3.3888	6.7776	10.1664	10	331
26.7412	13.3706	0.0534	5.9333	11.8666	17.7999	18	411

The Grain size (D) of the synthesized GO-NPs and interlayer distance can be calculated as shown in Table 2.

Table 2. Claculation of Material Parameters with the help of 2θ/⁰ values.

2θ/⁰	**FWHM [°2Th.]**	**Intensity counts**	**d-spacing [Å]**	**Grain size (D) (nm)**
10.8908	0.1979	100.00	4.99484	7.0382
20.1314	0.2303	26.09	4.24377	6.1148
26.7412	0.1279	20.00	3.33380	11.1431

It is obvious from above table that range of grain size was found to be 7.0382 nm at 2θ/⁰ = 10.8908 to 11.1431 nm at 2θ/⁰ = 26.7412 respectively.

3.2.2. RGO-ZnO nanocomposite

In XRD spectrum of RGO-ZnO nanocomposite, a weak and broad peak at 2θ/⁰= 10.9 indicating the reduction of GO into graphene and the disordered stacking of graphene sheet into the nanocomposite as shown in Figure 3.

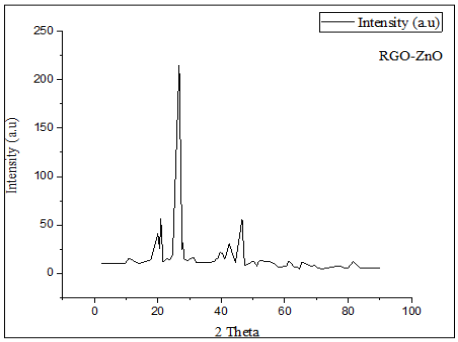

Fig. 3. XRD Pattern of RGO-ZnO Nanocomposite.

This diminished peak intensity at $2\theta^{/0}$= 10.9 in RGO-ZnO spectrum might be linked with the interactions between graphene and metal oxide [34]. Another prominent diffraction peak around at $2\theta^{/0}$=26 appears due to the shifting of GO into RGO-ZnO nanocomposite material [35]. The diffraction peak in Fig 3, situated at $2\theta^{/0}$=26 is substantially stronger than GO peak in Fig which may be due to the correlation of graphene with ZnO in a composite material.

Table 3. Claculation of Miller Indices through Xrd Diffraction Pattern of RGO-ZnO.

$2\theta^{/0}$	$\theta^{/0}$	$Sin^2\theta$	$1x \frac{Sin^2\theta}{Sin^2\theta_{min}}$	$2x \frac{Sin^2\theta}{Sin^2\theta_{min}}$	$3x \frac{Sin^2\theta}{Sin^2\theta_{min}}$	Whole integers	*Hkl*
10.8765	5.4382	0.0089	1	2	3	3	111
20.9333	10.4666	0.0330	3.7078	7.4156	11.1234	11	311
26.7832	13.3916	0.0536	6.0224	12.0448	18.0672	18	411
47.1460	23.5730	0.1599	17.9662	35.9324	53.8986	54	721

The XRD pattern of composite material indicates that material is well crystallized. In Fig 2, all $2\theta^{/0}$ values correspond to the formation phase of RGO-ZnO. The restacking of carbon sheet is prevented after the formation of composite material due to the formation of ZnO nano particles within its crystalline structure. The Grain size (D) of the synthesized composite material and interlayer distance can be calculated as shown in Table 4.

Table 4. Claculation of Material Parameters with the help of $2\theta^{/0}$ values.

$2\theta^{/0}$	FWHM [°2Th.]	Intensity counts	d-spacing [Å]	Grain size (D) (nm)
10.8765	0.1371	23.00	3.24410	10.1592
20.9333	0.2563	36.09	3.10321	5.4098
26.7832	0.1535	65.01	3.33772	9.2856
47.1460	0.3582	21.10	1.90864	4.2233

The range of grain size calculated was found in the range of 4.2233 nm at $2\theta/^0$ = 47.1460 to 10.1592 nm at $2\theta/^0$ = 10.8765 respectively.

3.3. DSC & TGA

TGA was used to analyze the reduction process from GO into RGO and to investigate the stability of synthesized material. DSC/ TGA curve of RGO-ZnO composite material is shown below:

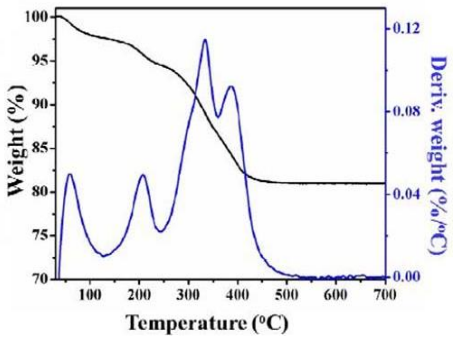

Fig. 4. DSC/ TGA of RGrO-ZnO Nanocomposite.

A combine plot of DSC/ TGA was obtained for the composite material in which sample was heated at temperature 700 ^{0}C by an increase of 10 ^{0}C temperature per minute in the air. Normally no decomposition essentially occurs after 700 ^{0}C, which is in perfect agreement with the report of Shamsuzzaman et al [36]. We know that thermal degradation and weight loss occurs by varying temperature [37]. In the above plot of RGO-ZnO, the main weight loss was noticed in the temperature range of 30-420 ^{0}C. Weight loss in temperature range of 30-150 ^{0}C might be due to moisture and solvent adsorbed between graphene layers in the composite material. Similarly the weight loss from 150-420 ^{0}C is due to the loss of oxygen-containing groups in GO. Unstable carbon remaining in structure and pyrolysis of oxygen functional groups in the main structure yield CO and CO_2 above 420 ^{0}C. From 450 ^{0}C to onward there is no further weight loss which confirms the complete conversion of nano composite into stable ZnO nanoparticles.

3.4. Photocatalytic activity of GO-ZnO Nanocomposite against organic dyes

Graphene based metal oxides show good photocatalytic properties. It is commonly observed that most dyes are resistant to photolytic degradation and mainly N-containing dyes such as MB show this behaviour. In this study, therefore, MB was chosen as a model contaminant along with RhB to evaluate the photocatalytic activity of synthesized material. Photocatlytic behaviour of GO-ZnO for the degradation and removal of organic dyes from industrial effluents can be studied by varying different factors like contact time, dosage concentration etc.

Percentage degradation of organic dye was calculated by using the relation,

$$\% \text{ age degradation} = [(A_0 - A_t) / A_0] \times 100$$

Where A_0 is absorbance of dye at initial stage and A_t is the absorbance of dye at time "t".

3.4.1. Time dependent Photocatalytic activity

The effect of contact time on degradation of organic dyes was examined in the range of 10 min to 180 min at room temperature while concentration of photocatalyst was kept constant. In order to study photocatalytic behaviour of GrO-ZnO nanocomposite, the photodegradation of Rh-B and MB utilizing synthesized nanocomposite photocatalyst were explored under UV light. The absorbance spectra of pure Rh-B, MB and with photocatalyst in UV light exposure are given bellow,

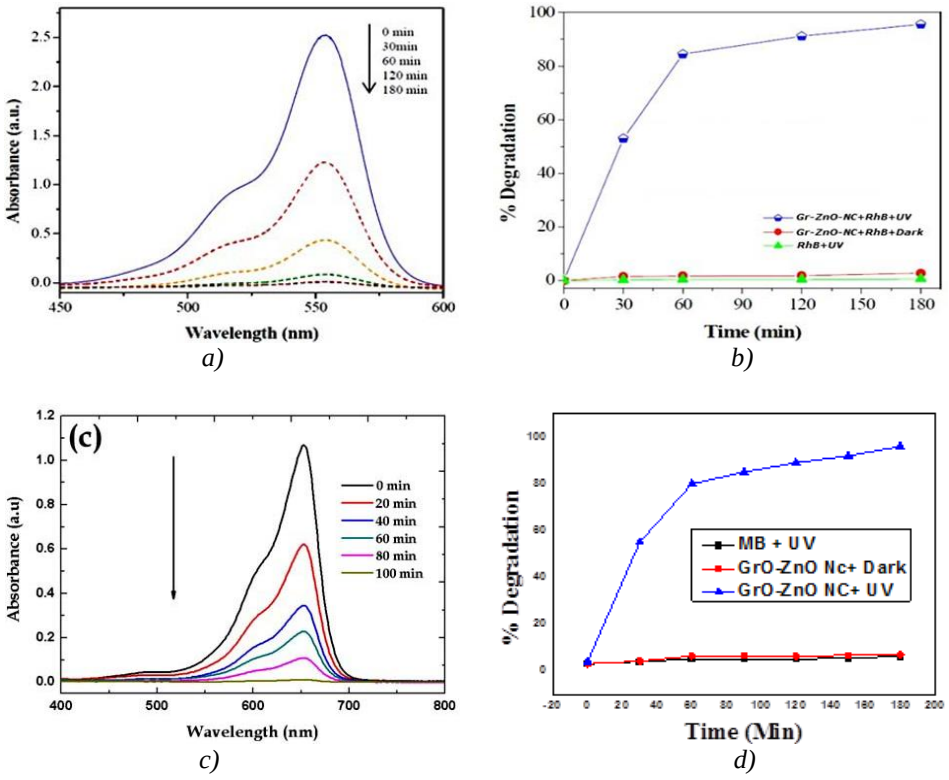

Fig. 5. Absorbance spectra and photodegradation pattern of RhB and MB; (a) Absorbance spectra showing time dependent photocatalysis of RhB dye on exposure of UV light; (b) Graph depicting RhB dye photodegradation by using GrO-ZnO NC; (c) Absorbance spectra showing time dependent photocatalysis of MB dye on exposure of UV light; (d) Graph depicting MB dye photodegradation by using GrO-ZnO NC.

Fig 5(a) and 5(c) show the UV-Vis absorption spectra of RhB, MB and removal efficiency of both these dyes without using synthesized materials under UV irradiation, darkness and by using GrO-ZnO nanocomposite in darkness and in the presence of UV irradiation are shown in Fig 5(b) and 5(d) respectively. GrO-ZnO in darkness and UV radiations alone did not show any significant adsorption of RhB and MB. The addition of GrO-ZnO into RhB solution and MB solution under UV light irradiation increased the removal efficiency after 180 min by up to 95% and 99%, respectively. It is obvious that photocatalytic degradation increases by increasing time. A comparison of results between the dark and light irradiation conditions clearly demonstrated that most of the dyes (RhB and MB) removal was due to photocatalytic degradation by the GrO-ZnO nanocomposite. Under UV conditions, there is a high removal efficiency of dyes because of the high photon energy in UV light and nanocomposite material also has a large surface area, that's why photodegradation could occur more strongly than in darkness or UV irradiation alone.

3.4.2. Effect of dosage concentration on Photocatalytic activity:

There is a regular increase in percentage degradation of RhB and MB by increasing dosage of photocatalyst from 1mg/L to 15mg/L as shown in Figure 6.

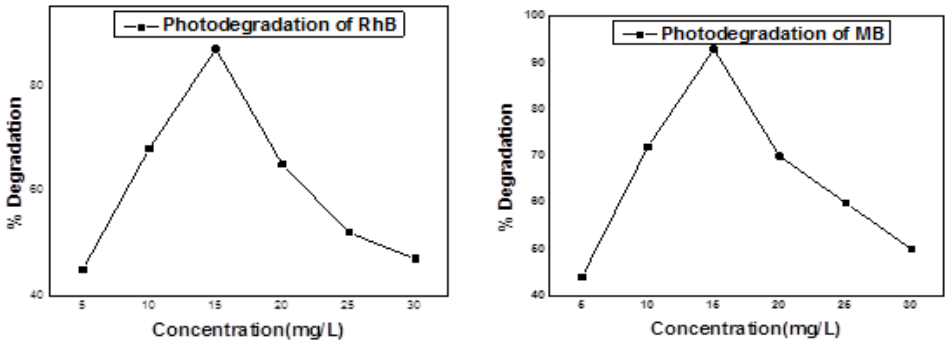

Fig. 6. Effect of dosage concentration on photodegradation of RhB and MB.

The increased GrO-ZnO nanocomposite dosage led to more active sites for adsorption and thus more moiety availability for photocatalytic degradation of RhB and MB molecules. The maximum percentage degradation efficiency recorded in case of RhB and MB was about 85% and 92% respectively. It was noticed in both cases that the removal efficiency of both dyes decreased as the dosage loading was increased above 15mg/L. The excessive increase in the amount of suspended nanocomposite material may disturb the penetration of visible light into the reaction system and cause considerable decrease in photo degradation process. Thus 15mg/L dosage of GO-ZnO was found to be most suitable for the removal of organic dyes i.e RhB and MB.

4. Conclusion

GO-ZnO nanocomposite was successfully synthesized by following Hummer's method. Different techniques including FTIR, XRD studies and TGA were utilized to study the properties of composite material and to confirm its formation. Synthesized material was used as a photocatalyst to remove RhB and MB dyes from their solutions. Removal efficiency of both dyes by using GO-ZnO as a photocatalyst was evaluated by varying time and dosage concentration. The optimum conditions for maximum removal efficiency of both organic dyes by using GO-ZnO nanocomposite as a photocatalyst was observed by giving 180 min contact time and 15mg/L dosage concentration.

Acknowledgments

The Authors would like to thank Lahore Garrison University to carry out this research project. We are also thankful to Comsat Institute of Information & Technology Lahore, Pakistan for assisting us in sample characterization.

References

[1] T. Robinson et al., Bioresource Technology **77**(3), 247 (2001).
[2] M. Mehra, T. R. Sharma, Advances in Applied Science Research **3**(2) 849 (2012).
[3] E. Fosso-Kankeu et al., Journal of Industrial and Engineering Chemistry **22**, 171 (2015).
[4] G. Crini, Bioresource technology **97**(9), 1062 (2006).
[5] R. Malik, D. S. Ramteke, S. R. Wate, Waste management **27**(9), 1 (2006).
[6] I. Arslan et al., Journal of Environmental Engineering **126**(10), 903 (2000).

[7] N. Stock et al., Environmental Science & Technology **34**(9), 1747 (2000).
[8] H. Karimi-Maleh et al., J. Mol. Liq. **314**, 113588 (2020).
[9] J. Abdi, H. Abedini, Chem. Eng. J. **400**, 125862 (2020).
[10] J. Abdi, N. M. Mahmoodi, M. Vossoughi, I. Alemzadeh, Microporous Mesoporous Mater. **273**, 177 (2019).
[11] N. M. Mahmoodi et al., Appl. Surf. Sci. **480**, 288 (2019).
[12] J. Abdi, M. Vossoughi, N. M. Mahmoodi, I. Alemzadeh, Chem. Eng. J. **326**, 1145 (2017).
[13] S. Z. N. Ahmad et al., Chem. Eng. Commun. **20**, 1 (2020).
[14] T. V. H. Tran, T. H. Cao, T. N. Pham, T. T. Pham, M. C. Le, J. Chem. **2019**, 1 (2019).
[15] F. Zhang, X. Chen, F. Wu, Y. Ji, Colloids Surf. A Physicochem. Eng. Asp. **509**, 474 (2016).
[16] G. J. F. Cruz et al., Water Sci. Technol. **2017**, 492 (2018).
[17] M. Zhang, L. Chang, Y. Zhao, Z. Yu, Arab. J. Sci. Eng. **44**, 111 (2019).
[18] R. Beura, S. Rajendran, M. A. Gracia Pinilla, P. Tangadurai, J. Water Process Eng. **32**, 100966 (2019).
[19] S. Rajendran, Sci. Rep. **6**, 31641 (2016).
[20] H. A. Sani, m. b. Ahmad, T. A. Saleh, RSC Adv. **6**, 108819 (2016).
[21] R. Salehi, M. Arami, N. M. Mahmoodi, H. Bahrami, S. Khorramfar, Colloids Surf. B Biointerfaces **80**, 86 (2010).
[22] M. Ghaedi, A. Ansari, M. H. Habibi, A. R. Asghari, J. Ind. Eng. Chem. **20**, 17 (2014).
[23] J. Qin et al., Mater. Lett. **189**, 156 (2017).
[24] R. Saravanan et al., J. Mol. Liq. **221**, 1029 (2016).
[25] W. S. Hummers Jr., R. E. Offeman, Journal of the American Chemical Society **80**(6) 1339 (1958).
[26] S. D. Perera, R. G. Mariano, K. Vu et al., ACS Catalysis **2**(6), 949 (2012).
[27] M. Saranya, G. Srishti, I. Singh, R. Ramachandran, C. Santhosh, C. Harish, T. M. Vanchinathan, M. BhanuChandra, A. N. Grace, Nanosci. Nanotechnol. Lett. **5**, 349 (2013).
[28] T. Tatsuma, S. Saitoh, P. Ngaotrakanwiwat, Y. Ohko, A. Fujishima, Langmuir **18**, 7777 (2002).
[29] J. Liu, X. Li, L. Dai, Adv. Mater. **18**, 1740 (2006).
[30] B. Smith, Infrared Spectral Interpretaion, A Systematic Approach, CRC Press: Washington; 1999.
[31] R. L. Peesole, L. D. Shield, I. C. McWillam, Modern Methods of Chemical Analysis, Wiley: New York, 1976.
[32] D. L. Pavia, G. M. Lampman, G. S. Kriz, J. R. Vyvyan, Introduction to Spectroscopy, 4th ed., Brooks/Cole: USA, 2008.
[33] B. Saravanakumar, R. Mohan, S. J. Kim, Mater. Res. Bull. **48**, 878 (2013).
[34] Benxia Li, Tongxuan Liu, Yanfen Wang, Zhoufeng Wang, J colloid and interface science **377**, 114 (2012).
[35] C. Zhang, J. Zhang, Y. Su, M. Xu, Z. Yang, Y. Zhang, Physica E **56**, 251 (2014).
[36] A. Mashrai Shamsuzzaman, H. Khanam, R. N. Aljawfi, Arabian J. Chem. **10**, S1530 (2017).
[37] V. Musat, A. Tăbăcaru, B. S. Vasile, V. A. Surdu, RSC Adv. **4**, 63128 (2014).